Seismic Optimization of a Novel Tuned Sloshing Damper for the Chilean Region Based on Life-cycle Cost Criteria

Rafael O. Ruiz
Ph.D. Candidate, Dept. of Civil and Environmental Engineering and Earth Sciences, Univ. of Notre Dame, Notre Dame, IN, U.S.A and Dept. of Structural & Geotechnical Engineering, Pontificia Universidad Catolica de Chile, Santiago, Chile

Alexandros A. Taflanidis
Associate Professor, Dept. of Civil and Environmental Engineering and Earth Sciences, Univ. of Notre Dame, Notre Dame, IN, U.S.A

Diego Lopez-Garcia
Associate Professor, Dept. of Structural & Geotechnical Engineering, Pontificia Universidad Catolica de Chile, and National Research Center for Integrated Natural Disaster Management CONICYT/FONDAP/15110017, Santiago, Chile

ABSTRACT: The design of a new liquid damper device is considered in this paper based on life-cycle criteria. This new device, called Tuned Liquid Damper with Floating Roof (TLD-FR) maintains the advantages of traditional Tuned Liquid Dampers (low cost, easy tuning, alternative use of water) while establishing a linear and generally more robust/predictable damper behaviour through the introduction of a floating roof. This behaviour can be characterized by four dimensional parameters that represent the design variables for the system and are all related to the tank geometry. A probabilistic framework is established to perform the design optimization considering seismic risk criteria specific to the Chilean region. Quantification of this risk through time-history analysis is considered and the seismic hazard is described by a stochastic ground motion model that is calibrated to offer hazard-compatibility with ground motion prediction equations available for Chile. Two different criteria related to life-cycle performance are utilized in the design optimization. The first one, representing overall direct benefits, is the life-cycle cost of the system, composed of the upfront TLD-FR cost and the anticipated seismic losses over the lifetime of the structure. The second criterion, focusing on the performance of building contents, is the peak acceleration with a specific probability of exceedance over the lifetime of the structure. A multi-objective optimization is therefore established and stochastic simulation is used to estimate all required risk measures, whereas a Kriging metamodel is developed to support an efficient optimization process.

1. INTRODUCTION

In the last decade the use of seismic protection devices in Chilean buildings has gained popularity not only for preventing damages but also for improving the performance related to building contents. Mass dampers are sometimes preferred to facilitate these goals with an increasing trend for incorporation even within new buildings. Recently, a new type of Tuned Liquid Damper (TLD) was introduced by Ruiz et al. (2014). The new device (Figure 1), called Tuned Liquid Damper with Floating Roof (TLD-FR) consists of a traditional TLD with the addition of a floating roof. Since the roof is much stiffer than water, it prevents wave breaking, hence making the response linear even at large wave amplitudes. The roof also makes possible the addition of supplemental devices with which the level of damping for the liquid motion can be substantially augmented.

Although it is well known that TLDs offer lower installation and maintenance cost than Tuned Mass Dampers (TMDs), proper comparison of such devices needs to consider the life-cycle performance over their entire lifetime, incorporating the different level of vibration suppression (and thus benefits from reduction of seismic losses) offered by each. A probabilistic framework is presented here to estimate and optimize the life cycle cost of Chilean buildings equipped with TLD-FRs. The seismic hazard is considered through a stochastic ground motion model that is calibrated (Vetter et al. 2014) to offer hazard-compatibility for the Chilean region. This is established by tuning the predictive equations in the model to ground motion prediction equations available for Chile (Boroschek and Contreras 2012).

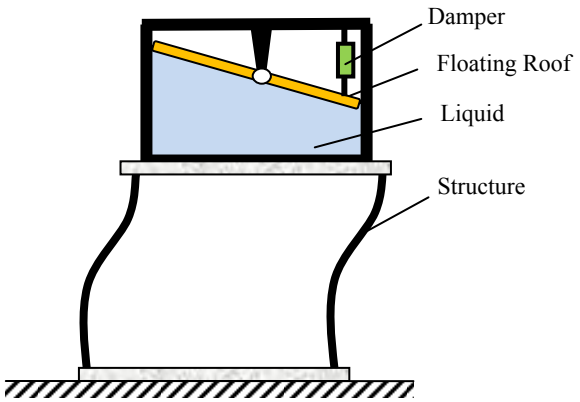

Figure 1: Tuned Liquid Damper with Floating Roof

Two different criteria related to the seismic risk are utilized in the design optimization. The first one, representing the direct benefits from the damper implementation, is the life-cycle cost of the system, composed of the upfront TLD-FR cost and the anticipated seismic losses over the lifetime of the structure. The upfront cost is related to the mass of the TLD-FR whereas the seismic losses are estimated by adopting an assembly-based vulnerability approach, utilizing the time-history response of the structure under the hazard provided by the aforementioned stochastic ground motion model. The second criterion, focusing on the performance of building contents, is the peak acceleration with a specific probability of exceedance over the lifetime of the structure. A multi-objective optimization is then established considering these two objectives and stochastic simulation is used to obtain all risk measures needed whereas a Kriging metamodel is developed to support an efficient optimization process. As an illustrative example the implementation of TLD-FR on a 20-story structure is considered and various interesting trends are investigated.

2. EQUATION OF MOTION FOR TLD-FR EQUIPPED STRUCTURE

2.1. TLD-FR equation of motion

The dynamic behaviour of the TLD-FR can be accurately described as linear (Ruiz et al. 2014) and through proper truncation approximated through a single degree of freedom model. A key point related to this behaviour is that not the entire liquid mass participates to the horizontal vibration response, something that ultimately reduces the efficiency of the device. Note that a similar remark holds for other type of liquid dampers, such as TLDs or liquid column dampers (Chang 1999). To better understand this TLD-FR behaviour one may consider its total mass to be distinguished to two masses (Ruiz et al. 2014): one that is rigidly attached to the tank walls (impulsive mass) and another one attached by a spring and a damper (convective mass).

Ultimately, the vibration characteristics for the TLD-FR depend on the tank geometry as well as the height of the liquid within the tank. A highly efficient numerical procedure, based on finite element principles for characterizing the motion of the liquid and on condensation of the vibratory response to the motion of the liquid-surface (Almazan et al. 2007), was recently presented by Ruiz et al. (2015) to describe this behaviour. Additionally, a proper non-dimensional analysis can be performed to derive a simplified parameterization of the equations of motion and relate them to only four parameters: three of them are the traditional parameters found used to describe TMD, the mass ratio r, the natural frequency ω_m and the damping ratio

ξ_m, while the fourth parameter is called efficiency index γ and is related to the amount of liquid that participates in the sloshing [a similar concept has been also discussed for liquid column dampers (Chang 1999)]. All these parameters can be related to the tank geometry through the aforementioned numerical procedure whereas for simplifying the design process a Kriging metamodeling approach was established in Ruiz et al. (2015) to obtain relationships that circumvent intensive finite element procedures.

The equations of motion for the TLD-FR are finally described as:

$$\ddot{\bar{\Gamma}} + 2\xi_m \omega_m \dot{\bar{\Gamma}} + \omega_m^2 \bar{\Gamma} = -\ddot{u}_b \qquad (1)$$

where $\ddot{u}_b$ represents the acceleration at the base of the TLD-FR and $\bar{\Gamma}$ corresponds to the normalized amplitude of the floating roof. The transmitted force F at the base of the TLD-FR, used to couple its behavior to the vibration of the structure it is placed upon, is:

$$F / m_{liq} = [\gamma\, 2\xi_m \omega_m]\dot{\bar{\Gamma}} + [\gamma\, \omega_m^2]\bar{\Gamma} - [1-\gamma]\ddot{u}_b \quad (2)$$

where m_{liq} is the total liquid mass. This transmitted force exhibits a dependence on the efficiency index, representing the part of the liquid that participates in the sloshing. An efficiency index equal to unity indicates that the whole liquid mass (m_{liq}) has a dynamic effect on the transmitted force, corresponding this case to that of a traditional Tuned Mass Damper (TMD). On the other hand, an efficiency index equal to zero indicates that the liquid moves together with the tank in a non-sloshing condition, and the liquid acts as a rigid body. This index can be controlled by Tank geometry (Ruiz et al. 2015).

2.2. Equation of motion for structure

Consider a n-degree of freedom structure with a TLD-FR located in a particular floor described through the location vector **L** (vector of zeros with a single 1, at the floor of the TLD-FR). Linear structural behavior is assumed here since it has been shown that for the Chilean region modern design/construction practices results in structures that demonstrate practically linear behavior even under strong excitations (EERI Special Earthquake Report 2010). The equation of motion for the structure under ground acceleration $\ddot{u}_g$ is then

$$\mathbf{M}_s\ddot{\mathbf{u}} + \mathbf{C}_s\dot{\mathbf{u}} + \mathbf{K}_s\mathbf{u} - \mathbf{L}^T F = -\mathbf{M}_s\mathbf{R}\ddot{u}_g \qquad (3)$$

where $\mathbf{M}_s$, $\mathbf{C}_s$ and $\mathbf{K}_s$ correspond to the mass, damping and stiffness matrices; while **R** is the vector of earthquake influence coefficients and **u** corresponds to the vector of displacements (relative to the ground) of each floor. The coupled system of equations for the structure equipped with a TLD-FR is then given by combining Eq. (3) and (1) with F for the former given by Eq. (2) and $\ddot{u}_b$ for the latter described as $\ddot{u}_b = \mathbf{L}\ddot{\mathbf{u}} + \ddot{u}_g$. A dimensional characterization of the damper can be then established by using $m_{liq} = r \cdot m_t$ and $\omega_m = f_m \cdot \omega_1$ where m_t is the total structural mass and ω_1 the fundamental structural frequency.

3. LIFE-CYCLE COST BASED DESIGN

The design of the TLD-FR is examined here considering life-cycle cost criteria. In particular a multi-objective formulation is examined following closely the concepts in (Gidaris et al. 2014).

3.1. Seismic risk quantification

Quantification of the life-cycle performance is established through the framework discussed in (Taflanidis and Beck 2009) and demonstrated in Figure 2. Approach relies of adoption of appropriate excitation, structural and performance evaluation models. The first provides the hazard, described in the form of time-histories for the ground acceleration. The second provides the structural response given that excitation and the third quantifies the favorability of that response in terms relevant to the structure stakeholders. The uncertainty in the parameters included in these model parameters, for example in the seismicity characteristics employed within the excitation model or in the damping characteristics for the structural model, is addressed adopting a probabilistic approach.

In this context let $\boldsymbol{\varphi} \in \Phi$ denote the n_φ-dimensional vector of TLD-FR design variables

and let $\boldsymbol{\theta} \in \Theta$, denote the n_θ-dimensional augmented vector of model parameters where Θ represents the space of possible model parameter values and Φ the admissible design space. Vector $\boldsymbol{\theta}$ is composed of all the model parameters for the individual structural system, excitation, and performance evaluation models. A probability density function (PDF) $p(\boldsymbol{\theta})$, is assigned to $\boldsymbol{\theta}$ based on our available knowledge. The risk is ultimately described the expected value of some risk-consequence measure under distribution $p(\boldsymbol{\theta})$, with different selections for that measure supporting different definitions for the risk. Here two different risk quantifications are considered.

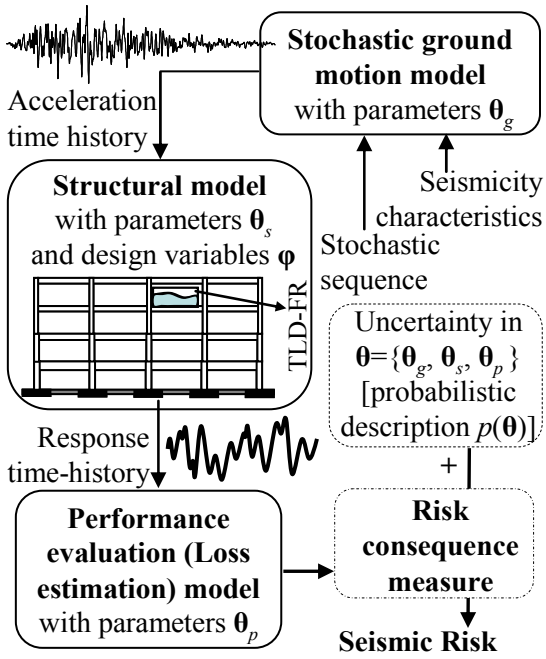

Figure 2: Schematic for risk quantification

The first, representing direct consequences, is the total life-cycle cost $C(\boldsymbol{\varphi})$, given by adding the initial cost $C_i(\boldsymbol{\varphi})$,which is a function of the dimensions of the TLD-FR, and the cost due to earthquake losses over the life-cycle of the structure $C_l(\boldsymbol{\varphi})$. The latter is dependent on earthquake losses per seismic event and on assumptions about occurrence rates for such events. For a Poisson assumption for occurrence of earthquakes (i.e., independent occurrence of seismic events), as considered in the example later, this risk consequence measure is given by:

$$h(\boldsymbol{\varphi},\boldsymbol{\theta}) = C_r(\boldsymbol{\varphi},\boldsymbol{\theta}) \nu t_{life} [(1-e^{-r_d t_{life}}) / r_d t_{life}] \quad (4)$$

where r_d is the discount rate, t_{life} is the life cycle considered and $C_r(\boldsymbol{\varphi},\boldsymbol{\theta})$ is the repair cost given the occurrence of an earthquake event. For estimating the latter an assembly-based vulnerability approach is adopted (Goulet et al. 2007). According to this approach the components of the structure are grouped into damageable assemblies, which consist of components of the system that have common vulnerability and repair cost characteristics (e.g. ceiling, wall partitions, etc.). Different damage states are designated to each assembly and a fragility function (quantifying the probability that a component has reached or exceeded its damage state) and repair cost estimates are established for each damage state. The former is conditional on some engineering demand parameter (*EDP*), which is related to peak characteristics for the structural response (e.g. peak interstory drift, peak floor acceleration, etc.). Combination of the fragility and cost information provides then $C_r(\boldsymbol{\varphi},\boldsymbol{\theta})$. The expected life-cycle losses $C_l(\boldsymbol{\varphi})$ for a given damper configuration is ultimately given by the expected value over the probability models for $\boldsymbol{\theta}$ as

$$C_l(\boldsymbol{\varphi}) = \int_\Theta h(\boldsymbol{\varphi},\boldsymbol{\theta}) p(\boldsymbol{\theta}) d\boldsymbol{\theta} \quad (5)$$

The second risk quantification examined, representing consequences to structural contents, is related to the peak acceleration a_p. Specifically the acceleration threshold a_{thresh} with a specific probability of exceedance over the life-cycle of the structure is adopted as the risk measure. Based on the Poisson assumption for the occurrence of seismic events, the probability of a_p exceeding a_{thresh} is

$$P[a_p > a_{thresh} \mid \boldsymbol{\varphi}, t_{life}] = 1 - \mathrm{e}^{-t_{life} \nu \cdot P[a_p > a_{thresh} \mid \boldsymbol{\varphi}, E_v]} \quad (6)$$

$$P[a_p > a_{thresh} \mid \boldsymbol{\varphi}, E_v] = \int_\Theta I_C(\boldsymbol{\varphi},\boldsymbol{\theta}) p(\boldsymbol{\theta}) d\boldsymbol{\theta} \quad (7)$$

where the risk consequence measure $I_C(\boldsymbol{\varphi},\boldsymbol{\theta})$ corresponds to the indicator function, which is one if $a_p(\boldsymbol{\varphi},\boldsymbol{\theta}) > a_{thresh}$ and zero if not. Eq. (7) gives the probability of exceeding the acceleration threshold given that a seismic event

has occurred, whereas Eq. (6) transforms that event-probability to probability of exceeding the threshold over the lifetime of the structure.

3.2. Ground motion modeling

Seismic hazard in the proposed framework (Figure 2) is described in terms of acceleration time-histories utilizing a stochastic ground motion modeling approach. This is established by modulating a stochastic sequence (typically white-noise) through functions that address spectral and temporal properties of the excitation (Papadimitriou 1990; Vetter et al. 2014). The parameters of these functions (for example strong ground motion duration or Arias intensity) are then related to seismicity characteristics (such as rupture distance r_{rup} and moment magnitude M) and site characteristics (such as shear wave velocity V_{s30}) through appropriate predictive relationships.

A recently published methodology (Vetter et al. 2014) is adopted here to select these relationships so that compatibility of the resultant ground motions to the regional hazard is established. The latter can be described through ground motion prediction equations (also references as attenuation relationships) that provide estimates of the spectral acceleration as a function of seismicity and site characteristics. The goal is then to tune a stochastic ground motion model to match these estimates for a specific structure (defined through the structural periods of interest) and a specific seismicity range (defined by selected values for M and r_{rup}). This ultimately corresponds to an optimization problem for selection of the predictive relationships in the ground motion model (Vetter et al. 2014). Though this approach a ground motion model that is specifically optimized to match the hazard for a specific location and structure is established. The versatile model initially proposed by Papadimitriou (1990) is chosen here as stochastic ground motion model, whereas the target seismic hazard is provided by predictive equations (GMPE) for Chile (Boroschek and Contreras 2012). Match is established for the peak spectral acceleration S_{pa} in period T range [0.75 1.3] s, chosen around the fundamental period of the structure of interest and for M and r_{rup} in ranges [6 9] and [50 250]km which are the ranges considered in the case study considered later. Figure 3 demonstrates the match established to the targeted hazard as well as a sample time-history provided by the proposed model.

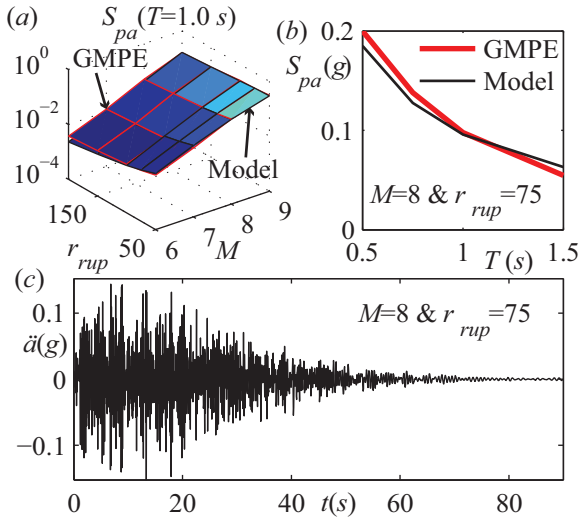

Figure 3: Results for ground motion modeling approach; match for targeted hazard for (a) different M-r_{rup} values for period T=1 s and (b) for different periods T for specific M-r_{rup} and (c) sample motion

3.3. Design optimization approach

The multi-objective design is expressed as

$$\boldsymbol{\varphi}^* = \arg\min_{\boldsymbol{\varphi}\in\Phi}\{C(\boldsymbol{\varphi}), a_{thresh}\}^T \quad \text{such that } P[a_p > a_{thresh} \mid \boldsymbol{\varphi}, t_{life}] = p_o \tag{8}$$

where $C(\boldsymbol{\varphi})$ [first objective] is the life-cycle cost and a_{thresh} [second objective] is the peak acceleration threshold with probability of being exceeded p_o over the lifetime of the structure. This multi-objective formulation leads ultimately to a set of points (also known as dominant designs) that lie on the boundary of the feasible objective space and they form a manifold, which is called Pareto front. A point belongs to the Pareto front and it is called Pareto optimal point if there is no other point that improves one objective without detriment to the other. The motivation behind the multi-objective

formulation of the problem is that the decision-maker (e.g. building owner) can choose among a range of TLD-FR configurations (Pareto optimal solutions) that describe different decision making attitudes towards risk in the context of the importance of reducing the risk associated with impact on the building contents (described here by peak acceleration).

For performing this optimization the probabilistic integrals in Eqs. (5) and (7) are required. They are both estimated here through stochastic simulation utilizing N samples from proposal density (importance sampling density) $q(\boldsymbol{\theta})$, leading to the following expressions

$$\hat{C}_l(\boldsymbol{\varphi}) = 1/N \sum_{j=1}^{N} h(\boldsymbol{\theta}^j) p(\boldsymbol{\theta}^j)/q(\boldsymbol{\theta}^j)$$
$$\hat{P}[a_p > a_{thresh} \mid \boldsymbol{\varphi}, \mathrm{E}_v] = \frac{1}{N}\sum_{j=1}^{N} I_C(\boldsymbol{\varphi}, \boldsymbol{\theta}^j)\frac{p(\boldsymbol{\theta}^j)}{q(\boldsymbol{\theta}^j)} \quad (9)$$

where $\boldsymbol{\theta}^j$ denotes the sample used in the j^{th} simulation. Furthermore for supporting an efficient optimization a surrogate modeling approach is adopted following the guidelines in Gidaris and Taflanidis (2015). A large set of design configurations (1000 in the case study discussed later) for the TLD-FR is established utilizing a latin hypercube sampling in Φ and both risk measures C_l and a_{thresh} are estimated for them. Using this information a Kriging metamodel is established to provide a highly efficient approximation to the system risk (thousands of evaluations within minutes) and this metamodel is then used within the optimization in Eq. (8).

4. CASE STUDY

For case study the design for a TLD-FR for a 20-story concrete shear-wall structure is considered. Details about the structural model may be found in (Steib 2011). Uncertainty is included in the structural mass and in the damping ratio. Both are modeled as Gaussian random variables with coefficient of variation 20% over their nominal values (reported in the previous reference). For the nominal model, i.e. corresponding to the median values of model parameters, the first three modes (and participation factors in parenthesis) are 1.09 sec (66%), 0.30 sec (17%) and 0.14 sec (7%). Fragility and repair cost information is included in Table 1, where the fragility function is a conditional cumulative lognormal distribution with median β_f and standard deviation σ_f. Note that damages to structural components are not included in this study since as discussed earlier are expected to have minimum contribution (behavior remains elastic even for stronger events). n_e in this table corresponds to the number of elements assumed per story whereas for each of the three different damageable assemblies different damage states are considered (total repair cost per assembly is obtained by considering the contribution from all damage states). The fragility and repair cost selections adopted follow the guidelines in (Gidaris and Taflanidis 2015).

Table 1. Characteristics for cost estimation

State	β_f	σ_f	n_e	\$/ n_e
Partitions				
Small	0.21%	0.60	1000m^2	22
Moderate	0.71%	0.45	1000m^2	60
Severe	1.20%	0.45	1000m^2	92
Contents				
Damage	0.70g	0.30	100	1500
Acoustical Ceiling				
Small	0.55g	0.40	2000m^2	15
Extensive	1.00g	0.40	2000m^2	120
Severe	1.50g	0.40	2000m^2	230

The total life-cycle cost for the structure is estimated as the sum of the repair cost due to the earthquake losses over the life-cycle of the structure and the initial cost of the TLD-FR. For the initial cost of the damper a simplified assumption is established here; the cost is assumed to depend linearly to the damper mass $C_i = b_c m_{liq}$ and three different cases are examined for this proportionality, b_c=[175 200 225] \$/ton.

For the seismic hazard the model discussed in Section 3.2 is utilized. Seismic events are assumed to occur following a Poisson distribution and so are independent of previous occurrences. The uncertainty in moment magnitude M is modeled by the Gutenberg-

Richter relationship truncated on the interval $[M_{min}, M_{max}] = [6.0, 9.0]$, (events smaller than M_{min} do not contribute to the seismic risk) which leads to $p(M) = b_M e^{-b_M M} / (e^{-b_M M_{min}} - e^{-b_M M_{max}})$ and expected number of events per year $\nu = e^{a_M - b_M M_{min}} - e^{a_M - b_M M_{max}}$, with the regional seismicity factors selected as b_M=0.8log$_e$(10) and a_M=4.00log$_e$(10), leading to ν=0.16 Regarding the uncertainty in the event location and orientation with respect to the fault, the closest distance to the fault rupture, r_{rup}, for the earthquake events is assumed to follow a beta distribution in [50 250] km with median r_{med} = 130 km and coefficient of variation 40%. Under these assumptions for the hazard the life-cycle cost and a_{thresh} for the uncontrolled structure are, respectively, \$1.58$x10^5$ and 0.71 g.

The analysis is performed for three different efficiency indexes. The optimization is then established over the remaining design variables (r, f_m and ξ_m). The ranges assumed for developing the Kriging metamodel are [0.5 2]% for r, [0 20]% for ξ_m and [0.92 1] for f_m. Due to the simplified assumption that the initial cost is related only to the total liquid mass (and not the exact tank geometry) incorporation of the efficiency index as a design variable was redundant since it is well-understood that larger efficiency index would yield better results (Ruiz et al, 2014) and therefore correspond to the optimal design. Results are reported in Figure 4 which shows the Pareto fronts for the different $\gamma$and b_c values. In the Pareto front the TLD-FR mass ratio under optimal design is also reported in some instances (extremes of the front) since this is the main design variable distinguished along the front (frequency and damping ratio simply take proper tuning values for that r). For the same extreme cases of the front the decomposition of the total cost (ratio) to upfront and repair cost is also shown (in parenthesis).

The results demonstrate that the TLD-FR can provide a considerable reduction for both C and a_{thresh} with the reductions in the latter being in general higher. As expected, larger values for the TLD-FR efficiency indexes yield better performance whereas reduction of the upfront cost for the damper also contributes to similar trends. In this case the optimal design corresponds to larger mass ratios (since upfront cost is reduced larger dampers can be adopted) which contributes to the better performance while also yielding a smaller distribution of the Pareto front. The efficiency index seems to also have a similar effect on reducing the spread of the Pareto front.

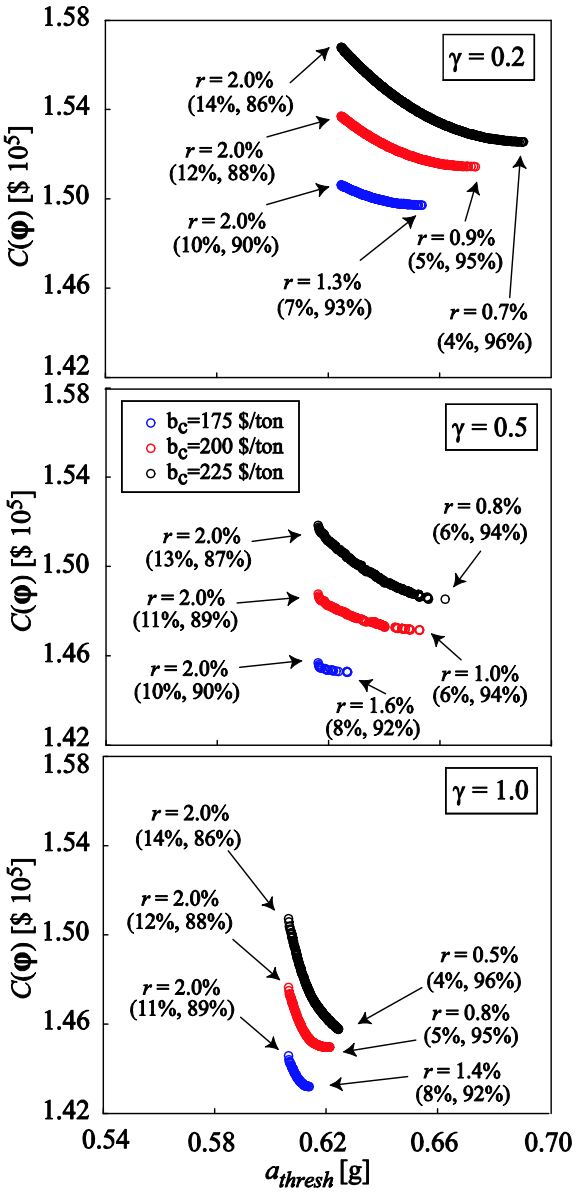

Figure 4: Pareto front curves life-cycle cost C and jerk threshold j_{thresh} with probability of exceedance p_o=10% in 50years, for different efficiency indexes γ (subplots) and different assumptions for upfront cost of dampers (curves in each subplot)

The stakeholder can ultimately make a choice then among the different candidate solutions along the Pareto front by prioritizing the different competing objectives. This ultimately boils down to selection of the damper mass; larger masses yield greater reduction of a_{thresh} but a larger overall life-cycle cost (due to increase of upfront cost). Based on the Pareto-optimal solution the tank geometry can be then chosen (Ruiz et al. 2015).

5. CONCLUSIONS

A risk-informed multi-objective design was discussed in this paper for the novel TLD-FR, considering two different risk quantifications, the total life-cycle cost and the acceleration threshold with specific probability of exceedance (representing damages to building contents). A simulation-based risk assessment framework was considered and the ground acceleration time-histories within this framework were provided by a stochastic ground motion model tuned to match the hazard for the Chilean region. A Kriging metamodel was adopted to support the design optimization. The illustrative example showcased the efficiency of the approach for providing stakeholders with different Pareto optimal solutions.

6. ACKNOWLEDGEMENTS

The authors would like to acknowledge the support of Vicerrectoria de Investigacion of the Pontificia Universidad Catolica de Chile and Ministerio de Educacion de Chile.

7. REFERENCES

Almazan, J.L., Cerda, F.A., De la Llera, J.C., and Lopez-Garcia, D. (2007). "Linear isolation of stainless steel legged thin-walled tanks." *Eng Struct*, 29(7), 1596-1611.

Boroschek, R., and Contreras, V. (2012). "Strong ground motion form the 2010 Mw 8.8 Maule Chile earthquake and attenuation relations for Chilean subduction zone interface earthquakes." *International Symposium on Engineering Lessons Learned from the 2011 Great East Japan earthquake*, March 1-4, Tokyo, Japan.

Chang, C. C. (1999). "Mass dampers and their optimal designs for building vibration control." *Eng Struct*, 21, 454-463.

EERI Special Earthquake Report (2010), *Learning from Earthquakes: The Mw 8.8 Chile Earthquake of February 27, 2010.*

Gidaris, I., and Taflanidis, A. A. (2015). "Performance assessment and optimization of fluid viscous dampers through life-cycle cost criteria and comparison to alternative design approaches." *B Earth Eng*, 13(4), 1003-1028

Gidaris, I., Taflanidis, A. A., and Mavroeidis, G. P. (2014). "Multi-objective design of fluid viscous dampers using life-cycle cost criteria." *10th National Conference in Earthquake Engineering*, Anchorage, AK.

Goulet, C. A., Haselton, C. B., Mitrani-Reiser, J., Beck, J. L., Deierlein, G., Porter, K. A., and Stewart, J. P. (2007). "Evaluation of the seismic performance of code-conforming reinforced-concrete frame building-From seismic hazard to collapse safety and economic losses." *Earth EngStruDyn*, 36(13), 1973-1997.

Papadimitriou, K. (1990). "Stochastic characterization of strong ground motion and application to structural response." *Report No. EERL 90-03*, California Institute of Technology, Pasadena, CA.

Ruiz, R., Lopez-Garcia, D., and Taflanidis, A. (2014). "An Innovative Type of Tuned Liquid Damper." *Proceedings of the Tenth U.S. National Conference on Earthquake Engineering*, Anchorage, AK.

Ruiz, R., Lopez-Garcia, D., and Taflanidis, A. (2015). "Tuned Liquid Damper with Floating Roof: A New Device to Control Earthquake-Induced Vibrations in Structures." *Proceedings of the XI Congreso Chileno de Sismologia e Ingenieria Sismica*, Santiago, Chile.

Steib, F. (2011), "Aceleracion de piso en edificios de hormigon armado estructurados en base a muros sometidos a excitaciones sísmicas." *Master thesis,* Pontificia Universidad Catolica de Chile.

Taflanidis, A. A., and Beck, J. L. (2009). "Life-cycle cost optimal design of passive dissipative devices." *StructSaf*, 31(6), 508-522.

Vetter, C., Taflanidis, A., and Mavroeidis, G. (2014). "Development of ground motion models compatible with ground motion prediction equations." *Proceedings of the Tenth U.S. National Conference on Earthquake Engineering*, Anchorage, AK.